A Robustly Stable PI Controller For The Doubly-Fed Induction Machine

Carles Batlle
MA4, EPSEVG and IOC,
Universitat Politècnica de Catalunya
Vilanova i la Geltrú, 08800, Spain
carles.batlle@upc.edu

Arnau Dòria-Cerezo
EE, EPSEVG and IOC,
Universitat Politècnica de Catalunya
Vilanova i la Geltrú, 08800, Spain
arnau.doria@upc.edu

Romeo Ortega
Laboratoire des Signaux et Systmes,
Suplec
Gif-sur-Yvette, 91192, France
romeo.ortega@lss.supelec.fr

Abstract— **In this paper we propose a new control scheme for the doubly–fed induction machine (DFIM) that offers significant advantages, and is considerably simpler, than the classical vector control method. In contrast with the latter, where the DFIM is represented in a stator flux–oriented frame, we propose here a model with orientation of the stator voltage. This allows for an easy decomposition of the active and reactive powers on the stator side and their regulation—acting on the rotor voltage—via stator current control. Our main contribution is the proof that a linear PI control around the stator currents ensures global stability for a feedback linearized DFIM, provided the gains are suitably selected. The feedback linearization stage requires only measurement of the rotor and stator currents, hence is easily implementable. Finally, an outer loop control for the mechanical speed is introduced. The complete control system is tested both in simulations and experiments, showing good transient performance and robustness properties.**

I. Introduction

Doubly–fed induction machines (DFIM) have become very popular for renewable energy applications lately. They have been proposed in the literature, among other applications, for wind-turbine generators [11],[14], hybrid engines [5] or high performance storage systems [1], [3]. The attractiveness of the DFIM stems primarily from its ability to handle large speed variations around the synchronous speed (see [12] for an extended literature survey and discussion). Another advantage is that the power electronic equipment to control the machine only has to handle a fraction (maximum $20-30\%$) of the total power [13], reducing the losses (and the cost) of the power electronic converter.

Most DFIM controllers proposed in the literature are based on vector control and decoupling [10], see examples in [11], [15]. This methodology is based on the description of the electrical part of the DFIM in a new reference frame (usually the stator flux), which allows the decoupling of the active and reactive power of the stator side and their independent control through the rotor currents. To achieve the stator flux orientation the flux angle must be computed and several complicated (and fragile) rotation operations implemented. Other control schemes with rigorous stability and robustness analysis reported in the literature are the output feedback algorithm presented in [12], and the passivity–based controllers proposed in [3], [4].

This paper presents a new control algorithm for the DFIM that offers significant advantages, and is considerably simpler, than the previous control methods. In contrast with vector control, where the DFIM is represented in a stator flux–oriented frame, we propose here a model with orientation of the stator voltage. This allows for an easy decomposition of the active and reactive powers on the stator side and their regulation—acting on the rotor voltage—via stator current control. Our main contribution is the proof that a linear PI control around the stator currents ensures global stability for a feedback linearized DFIM—provided the gains are suitably selected. The feedback linearization stage requires only measurement of the rotor and stator currents, hence is easily implementable. Tuning rules for the PI gains are also provided, in particular, we prove that, if the integral gain is small, the proportional gain can take arbitrarily large values. Also, we prove the existence of large (open) regions in the controller parameter plane where stability is preserved. Finally, as done also in vector control, an outer loop control for the mechanical speed is introduced. The complete control system is tested both in simulations and in experiments, showing good transient performance and robustness properties.

II. DFIM Model

We start from the three phase dynamical equations of a DFIM, and assume that the machine is symmetric (all windings are equal), the stator-rotor cross inductances are smooth, sinusoidal functions of the rotor angle with just the fundamental term [6], [9], and that the three phase system is equilibrated. These assumptions allow the use of transformations, which greatly simplifies the control problem. The transformations (also known as Blondel–Parks transformations) are widely used in the study of power systems [9]. This mathematical transformation is used to decouple one of the (balanced) phases, to refer all variables to a common reference frame, and to obtain constitutive laws (stator–rotor cross inductances) independent of the relative angle between rotor and stator.

Similarly to [3], in this paper we propose a transformation to a synchronous frame rotating at the frequency of the stator voltage of the DFIM, which is assumed constant. This yields

$$\begin{aligned}\dot{\lambda}_s &= -(\omega_s L_s J_2 + R_s I_2) i_s - \omega_s L_{sr} J_2 i_r + v_s \quad (1)\\ \dot{\lambda}_r &= -(\omega_s - \omega) L_{sr} J_2 i_s \\ &\quad -[(\omega_s - \omega) L_r J_2 + R_r I_2] i_r + v_r \quad (2)\\ J\dot{\omega} &= L_{sr} i_s^T J_2 i_r - B_r \omega - \tau_L \quad (3)\end{aligned}$$

where λ_s, $\lambda_r \in \mathbb{R}^2$ are the stator and rotor fluxes, i_s, $i_r \in \mathbb{R}^2$ are the stator and rotor currents, $v_s = \mathrm{col}(V_s, 0) \in \mathbb{R}^2$, with V_s the amplitude of the three-phase stator voltage, is the stator voltage, the rotor voltage $v_r \in \mathbb{R}^2$ is the control input, ω is the mechanical speed, and ω_s is the stator frequency. R_s, R_r are the stator and rotor resistances, L_s, L_r and L_{sr} are the stator, rotor and self–inductances, with $L_s L_r > L_{sr}^2$, J is the inertia, B_r is the friction coefficient, τ_L is an external constant torque, and we defined the matrices

$$J_2 = \begin{bmatrix} 0 & -1 \\ 1 & 0 \end{bmatrix} \quad I_2 = \begin{bmatrix} 1 & 0 \\ 0 & 1 \end{bmatrix}. \quad (4)$$

Linking fluxes, $\lambda = \mathrm{col}(\lambda_s, \lambda_r)$, and currents, $i = \mathrm{col}(i_s, i_r)$, are related by

$$\lambda = \begin{bmatrix} L_s I_2 & L_{sr} I_2 \\ L_{sr} I_2 & L_r I_2 \end{bmatrix} i. \quad (5)$$

Following standard convention we partition all electrical signals into their, so–called, d and q components. For instance, the stator current is decomposed as $i_s = \mathrm{col}(i_{sd}, i_{sq})$. The use of the synchronous frame allows us to express the stator active and reactive powers in terms of i_{sd} and i_{sq}, respectively. In particular, assigning a desired value, i_{sq}^*, allows to compensate the power factor of the stator side of the machine, while i_{sd}^* can be used to control the active power (delivered or consumed) by the DFIM. In a drive application, we can fix i_{sd}^* as a desired value to achieve the target speed. In this paper we concentrate only on the problem of robust regulation of i_s to its desired value and refer the interested reader to [3] for further details on the power flow control policy and the determination of the equilibria.

III. Overall Control Scheme

The proposed control scheme is presented in Figure 1, where the current control block assures stability of the electrical subsystem and an outer–loop control is added for speed regulation. As indicated above, in this paper we concentrate on current control and will prove that, after a basic feedback linearization stage, the current can be globally regulated with a PI around the stator currents with some suitably selected gains.

The transformation of the three phase (stator and rotor) currents to the synchronous–reference (aligned to the stator voltages) is achieved with the rotation matrices

$$K(\theta, \delta) = \begin{bmatrix} e^{J_2 \delta} & O_2 \\ O_2 & e^{J_2(\delta - \theta)} \end{bmatrix}$$

where δ is an arbitrary function of time that, for convenience, we select as $\dot{\delta} = \omega_s$. Notice that this part of the scheme is easier to implement than vector control, which requires stator flux estimation.

IV. Current Controller

The proposed controller consists of a feedback linearization stage

$$v_r = (\omega_s - \omega) L_{sr} J_2 i_s + [(\omega_s - \omega) L_r J_2 + R_r I_2] i_r + u \quad (6)$$

and a PI action

$$u = -k_P J_2 \tilde{i}_s + k_I J_2 \int \tilde{i}_s dt. \quad (7)$$

with the scalar gains $k_P > 0, k_I \geq 0$, and we defined the error terms $\tilde{(\cdot)} = (\cdot) - (\cdot)^*$, where $(\cdot)^*$ is the constant desired value—e.g., an equilibrium point. (The reader is referred to [3] for further details on the definition of the latter.)

We attract the readers attention to the following important remarks:

R1. The first two terms in (6) exactly cancel the terms in (2), feedback linearizing the system and transforming the rotor equation into $\dot{\lambda}_r = u$.

R2. Due to the feedback linearization the overall system consists of a cascade of the electrical and the mechanical sub–systems. As the latter is a simple stable linear system, convergence to the equilibria of the electrical sub–system will imply stability of the complete dynamics.

R3. In contrast to standard practice, we have defined the PI, (7), with the skew–symmetric matrix J_2. Notice also the selection of the signs. These two features will be critical for the stability analysis.[1]

To carry out the stability analysis, we find convenient to express the closed–loop system in an alternative form. Replacing (6) and (7) in (1), (2), and using the definition of equilibria, we can write the closed–loop system in error coordinates as

$$\begin{aligned}\dot{\tilde{\lambda}}_s &= -(\omega_s L_s J_2 + R_s I_2) \tilde{i}_s - \omega_s L_{sr} J_2 \tilde{i}_r \quad (8)\\ \dot{\tilde{\lambda}}_r &= -k_P J_2 \tilde{i}_s + k_I J_2 \int \tilde{i}_s dt. \quad (9)\end{aligned}$$

Now, using the relation between fluxes and currents, (5), we get

$$\begin{aligned}\dot{\tilde{\lambda}}_s &= L_s \dot{\tilde{i}}_s + L_{sr} \dot{\tilde{i}}_r \\ &= L_s \dot{\tilde{i}}_s + \frac{L_{sr}}{L_r} (\dot{\tilde{\lambda}}_r - L_{sr} \dot{\tilde{i}}_s).\end{aligned}$$

[1] As explained in [7] this controller was obtained applying passivity–based nonlinear control techniques, but here we restrict ourselves to its analysis.

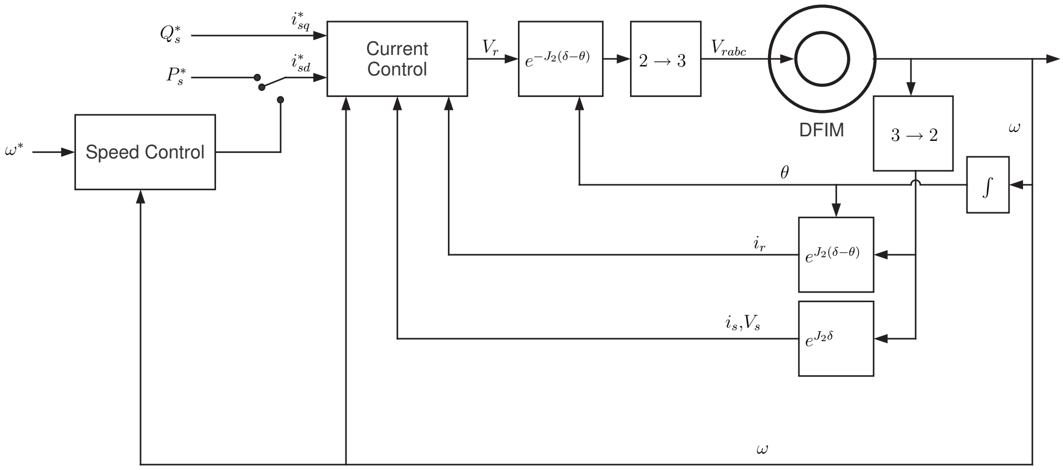

Fig. 1. Control scheme for a DFIM.

Similarly $\tilde{i}_r = \frac{1}{L_r}(\tilde{\lambda}_r - L_{sr}\tilde{i}_s)$. Replacing the last two equations in (8), differentiating and using (9) we can write the electrical dynamics in the equivalent form

$$D(p)\tilde{i}_s = 0, \tag{10}$$

with the polynomial matrix, in the derivative operator $p = \frac{d}{dt}$,

$$D(p) = p^3 I_2 + (c_1 I_2 + c_2 J_2)p^2 + (c_3 I_2 + c_4 J_2)p + c_5 I_2,$$

and the parameters

$$c_1 = \frac{R_s L_r}{\mu}, \quad c_2 = \omega_s - \frac{L_{sr}}{\mu} k_P, \quad c_3 = \frac{\omega_s L_{sr}}{\mu} k_P,$$

$$c_4 = -\frac{L_{sr}}{\mu} k_I, \quad c_5 = \frac{\omega_s L_{sr}}{\mu} k_I,$$

where $\mu = L_s L_r - L_{sr}^2 > 0$.

Equation (10) describes, of course, a linear system of order six whose stability is determined by the characteristic polynomial $\det D(s)$, with $s \in \mathbb{C}$ the Laplace transform variable. Although the study of this (sixth–order) polynomial can be carried out with classical tools, e.g., Routh–Hurwitz criterion, this procedure yields complex parameter relations that complicate the choice of the PI gains. On the other hand, we show now that the particular structure chosen for the PI, see R3 above, permits very simple analysis and tuning rules and ensures some interesting robustness properties. These results are contained in the following proposition, whose proof is given in Appendix.

Proposition 1: Consider the DFIM system (1)–(3) in closed–loop with the control (6) and (7).

P1. If $k_I = 0$, for all $k_P > 0$, the electrical coordinates converge to their desired values, while the speed is bounded and also converges.

P2. There exists $k_I^M > 0$ such that, for all $k_I \in (0, k_I^M]$ and all $k_P > 0$, the electrical coordinates converge to their desired values, while the speed is bounded and also converges.

Let us briefly explain the motivation behind the proposed PI (7). Towards this end, we attract the readers attention to the coefficients c_2 and c_3, that depend on k_P. Due to the particular choice of the proportional gain matrix we have that $c_3 > 0$. On the other hand, even though c_2 may become negative (for large values of k_P), this coefficient multiplies the skew–symmetric matrix J_2. To understand how this influences the stability let us consider first the case $k_I = 0$. The dynamics of the system is then described by $D_0(p)\tilde{i}_s = 0$, with

$$D_0(p) = p^2 I_2 + (c_1 I_2 + c_2 J_2)p + c_3 I_2.$$

It turns out that system is asymptotically stable for all $k_P > 0$. Indeed, consider a Lyapunov function candidate

$$V(\tilde{i}_s, \dot{\tilde{i}}_s) = \frac{1}{2}|\dot{\tilde{i}}_s|^2 + \frac{c_3}{2}|\tilde{i}_s|^2,$$

with $|\cdot|$ the Euclidean norm. Notice that, since $c_3 > 0$ this is a positive definite function. Taking the derivative of V we get

$$\dot{V} = -c_1|\dot{\tilde{i}}_s|^2 \leq 0,$$

which proves the claim. Observe that, since c_2 disappears in the computation of the derivative, its sign may be positive or negative without affecting the conclusion. This nice stability property is lost if the proportional gain matrix is not skew–symmetric.

A similar argument can be used to justify the choice of the integral gain matrix, as follows. The characteristic equation of the closed–loop system has the following form

$$\det D(s) = s^6 + as^5 + bs^4 + cs^3 + ds^2 + es + f \tag{11}$$

where

$$\begin{aligned}
a &= \frac{1}{\mu}2L_rR_s \\
b &= \frac{1}{\mu^2}(\omega_s^2\mu^2 + L_{sr}^2k_P^2 + L_r^2R_s^2) \\
c &= \frac{1}{\mu^2}2L_{sr}k_P(R_sL_r\omega_s + L_{sr}k_I) = c_0 + k_Ic_1 \\
d &= \frac{1}{\mu^2}L_{sr}(\omega_s^2L_{sr}k_P^2 + L_{sr}k_I^2 + 2L_r\omega_sR_sk_I) \\
&= d_0 + k_Id_1 + k_I^2d_2 \\
e &= \frac{1}{\mu^2}2L_{sr}^2\omega_s^2k_Pk_I = k_Ie_1 \\
f &= \frac{1}{\mu^2}L_{sr}^2\omega_s^2k_I^2 = k_I^2f_2
\end{aligned}$$

where we have factored the gain k_I. Thus,

$$\begin{aligned}
\det D(s) &= s^6 + as^5 + bs^4 + c_0s^3 + d_0s^2 \\
&\quad + k_I(c_1s^3 + d_1s^2 + e_1s) + k_I^2(d_2s^2 + f_2).
\end{aligned}$$

For small k_I the quadratic term can be disregarded and we can analyze the the reduced polynomial

$$\beta(s)s + k_I\alpha(s) = 0$$

where

$$\begin{aligned}
\beta(s) &= s^4 + as^3 + bs^2 + c_0s + d_0 \\
\alpha(s) &= c_1s^2 + d_1s + e_1.
\end{aligned}$$

Notice that $\beta(s)$ is the characteristic polynomial of the system with $k_I = 0$, therefore its roots are always on the open left–half plane. On the other hand, the roots of $\alpha(s)$, given by,

$$s_1, s_2 = -\frac{d_1}{2c_1} \pm \sqrt{\left(\frac{d_1}{2c_1}\right)^2 - \frac{e_1}{c_1}} \tag{12}$$

have negative real part for $e_1, c_1 > 0$—which is true in our case. This analysis, combined with a continuity argument, provides a proof of claim P2 in Proposition 1.

Before closing this section we make the following remark. The result of Proposition 1 concerns stability of the closed-loop system for any k_P (even arbitrarily large) and for k_I small enough. In fact, an asymptotic analysis of the Routh–Hurwitz conditions for the characteristic polynomial, $\det D(s)$, shows that there is an unbounded region in the first quadrant, below $k_I = \frac{L_rR_s}{\mu}k_P - \frac{L_rR_s}{L_{sr}}\omega_s$, where the closed-loop system is stable; details may be found in [7].

V. Simulations

In this section we implement a numerical simulation of the controller scheme developed in the previous sections. We use the following DFIM parameter values: $R_s = 4.92\Omega$, $R_r = 4.42\Omega$, $L_s = 7.25$mH, $L_r = 7.15$mH, $L_{sr} = 7.1$mH, $J_m = 0.00512$Kgm^2, $B_r = 0.005$N m s rad^{-1}.

As indicated in the previous section, the mechanical speed dynamics (3) can be stabilized by means of

$$\begin{aligned}
i_{sd}^* &= \frac{1}{L_{sr}i_{rq}^*}\Big(L_{sr}i_{sq}^*i_{rd}^* - B_r\omega^* - \tau_L - \\
&\quad + k_{\omega P}(\omega - \omega^*) + k_{\omega I}\int(\omega - \omega^*)dt\Big)
\end{aligned} \tag{13}$$

yielding the closed–loop behavior

$$J\dot{\omega} = -B_r(\omega - \omega^*) - k_{\omega p}(\omega - \omega^*) - k_{\omega i}\int(\omega - \omega^*)dt + \epsilon_t,$$

where $\epsilon_t \to 0$ exponentially fast. Notice that the first three (constant) terms in (13) can be disregarded in a practical implementation, as their effect will be compensated by the integral part in any case.

The controller gains were fixed as $k_P = 10$, $k_I = 2$, $k_{\omega P} = 1$ and $k_{\omega I} = 25$. Simulations start with a desired mechanical speed $\omega^* = 310$rad s^{-1} and at $t = 0.5$s the desired value is changed to $\omega^* = 325$rad s^{-1}. The desired q-stator current is fixed at $i_{sq}^* = 0$ in order to obtain a good power factor in the stator side.

Figure 2 shows the behavior of the mechanical speed. The transient can be improved by means of the control gain of (13) and the integral term brings the mechanical speed to the desired value. Figure 3 shows the behavior of the stator currents.

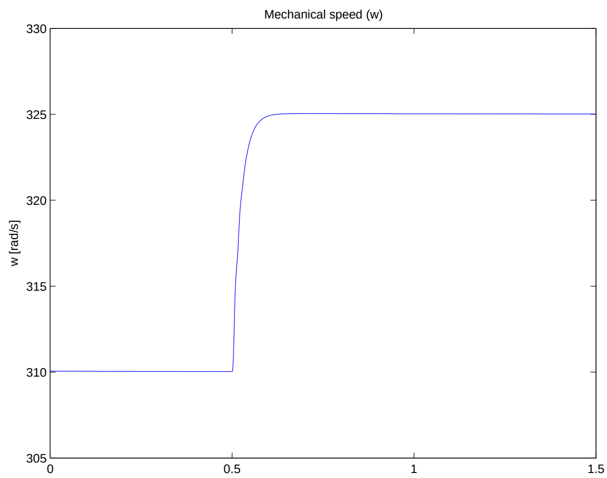

Fig. 2. Simulation results: mechanical speed, ω.

VI. Experimental Results

For the experimental setup we used a 1.1kW, 380/220V, 50Hz 2-poles machine, with the following parameters: $R_s = 4.92\Omega$, $R_r = 4.42\Omega$, $L_s = 7.25$mH, $L_r = 7.15$mH, $L_{sr} = 7.1$mH, star shape stator and rotor connection, $J_m = 0.00512$Kgm^2, $B_r = 0.005$N m s rad^{-1} and $\tau_L = 0$.

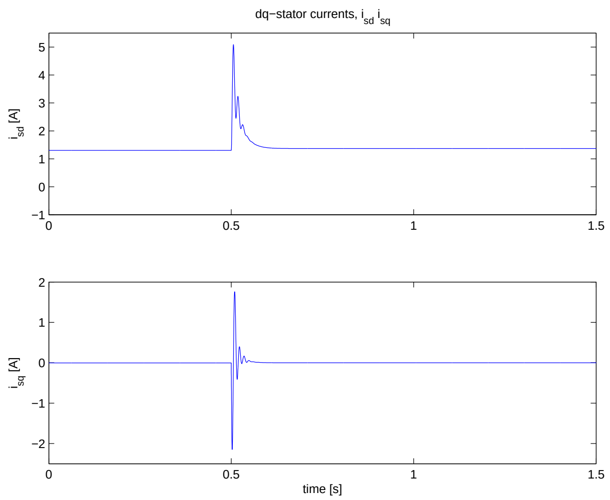

Fig. 3. Simulation results: dq-stator currents, i_{sd} and i_{sq}.

The three-phase rotor PWM voltages are generated by a bidirectional back-to-back converter[2]. The control algorithm is computed in a PC running with RTiC-Lab (Real Time Controls Laboratory) for Linux, with a 10kHz running time.

The experimental test consist in speeding up the machine from $\omega = 310\text{rad s}^{-1}$ to $\omega = 325\text{rad s}^{-1}$ and coming back to $\omega = 310\text{rad s}^{-1}$, and at the same time controlling the reactive power of the machine through i_{sq}. Experimental results are shown in Figures 4 to 8.

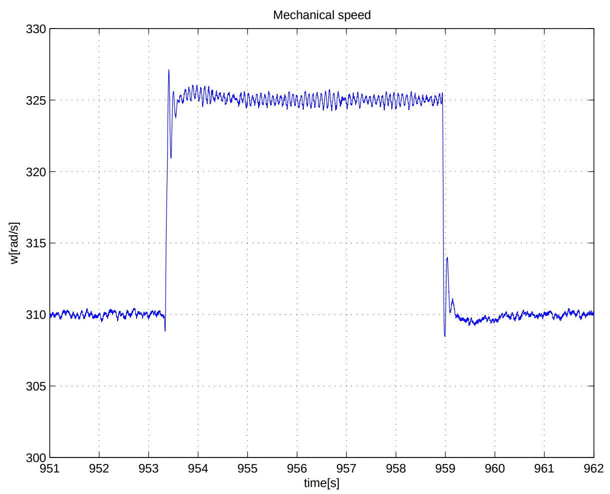

Fig. 4. Experimental results: mechanical speed ω.

In Figure 4 the mechanical speed is depicted. Figure 5 shows the dq-stator currents. Notice that i_{sq} remains close to zero, which means that the power factor of the stator side is very small, see also Figure 6. Finally, in Figures 7 and 8 the control action u_r and its corresponding a-phase are depicted.

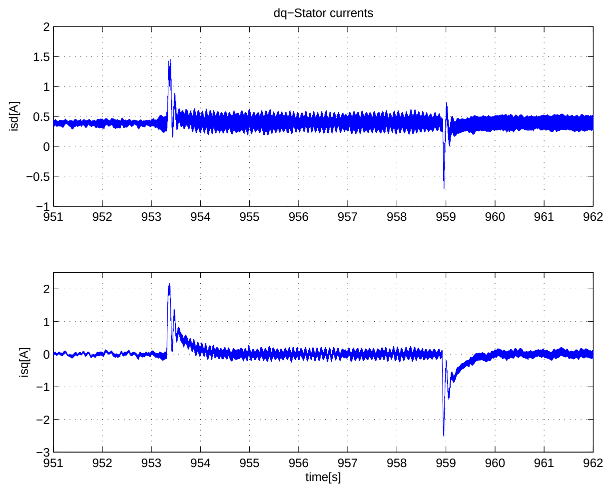

Fig. 5. Experimental results: dq-stator currents, i_{sd} and i_{sq}.

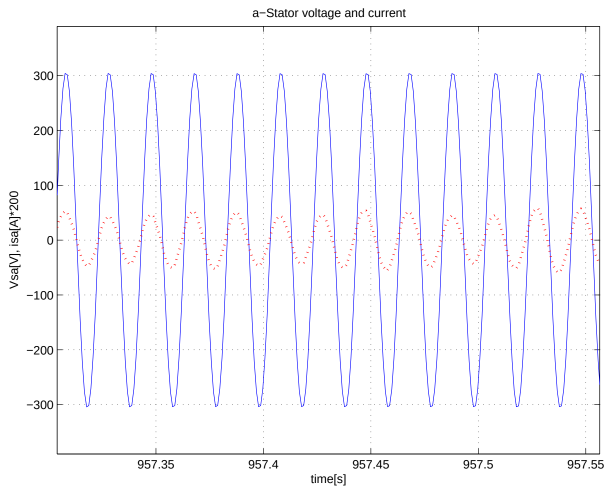

Fig. 6. Experimental results: a-stator voltage and current, v_{sa} and i_{sa}.

VII. Conclusions

In this paper a particularly simple controller for DFIM was presented. It consists of a feedback linearizing term and a PI around stator currents. We prove that the scheme is globally asymptotically stable for all values of the proportional gain and sufficiently small integral gains. As no stator flux estimation is required, the algorithm scheme is simpler than the classical vector control. Simulations and experiments were used to validate the control.

Acknowledgments

CB and ADC partially supported by the CICYT project DPI2004-06871-CO2-02.

References

[1] H. Akagi and H. Sato. Control and performance of a doubly-fed induction machine intended for a flywheel energy storage system. *IEEE Trans. Power Electron.*, 17(1):109–116, 2002.

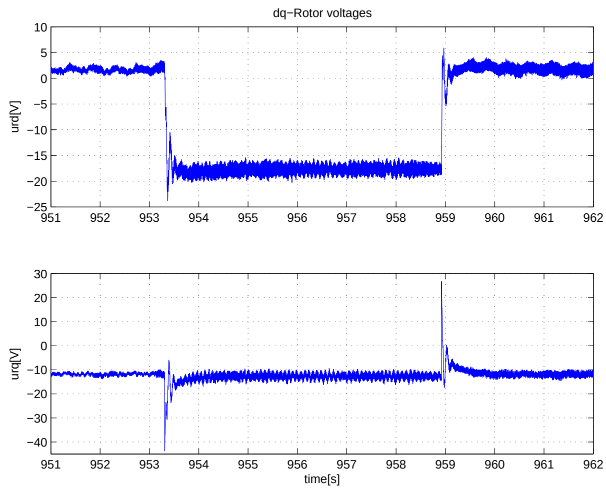

Fig. 7. Experimental results: dq-rotor voltages, v_{rd} and v_{rq}.

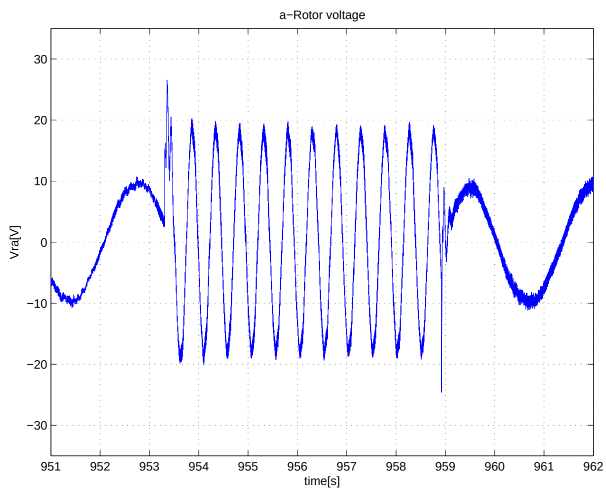

Fig. 8. Experimental results: a-rotor voltage, v_{ra}.

[2] C. Batlle, A. Dòria-Cerezo, and E. Fossas. IDA-PBC controller for a bidirectional power flow full-bridge rectifier. In *IEEE Proc. Conference on Decision and Control*, 2005.

[3] C. Batlle, A. Dòria-Cerezo, and R. Ortega. Power Flow Control of a Doubly–Fed Induction Machine Coupled to a Flywheel. *European Journal of Control*, 11(3):209–221, 2005.

[4] M. Becherif, R. Ortega, E. Mendes, and S. Lee. Passivity-based control of a doubly-fed induction generator interconnected with an induction motor. In *IEEE Proc. Conference on Decision and Control*, 2003.

[5] P. Caratozzolo, E. Fossas, J. Pedra, and J. Riera. Dynamic modeling of an isolated motion system with DFIG. In *Proc. CIEP*, pages 287–292, 2000.

[6] J. Chiasson. *Modeling and High Performance Control of Electric Machines*. John Wiley & Sons Inc., 2005.

[7] A. Dria-Cerezo. *Modeling, simulation and control of a doubly-fed induction machine controlled by a back-to-back converter.* PhD thesis, Universitat Politcnica de Catalunya, 2006.

[8] P.V. Kokotovic, H.K. Khalil, and J. O'Reilly. *Singular Perturbation Methods in Control: Analysis and Design*. Classics in Applied Mathematics. SIAM, 1999.

[9] P. C. Krause. *Analysis of electric machinery*. McGraw-Hill, 1986.

[10] W. Leonard. *Control of electric drives*. Springer, 1995.

[11] R. Peña, J. C. Clare, and G. M. Asher. Doubly fed induction generator using back-to-back pwm converters and its application to variable speed wind-energy generation. In *IEEE Proc. Electric Power Applications*, volume 143-5, pages 231–241, 1996.

[12] S. Peresada, A. Tilli, and A. Tonelli. Power control of a doubly fed induction machine via output feedback. *Control Engineering Practice*, 12:41–57, 2004.

[13] A. Petersson. *Analisys, modeling and control of doubly-fed induction generators for wind turbines.* PhD thesis, Chalmers University of Technology, Sweden, 2005.

[14] J.G. Slootweg, H. Polinder, and W.L. Kling. Dynamic modelling of a wind turbine with doubly fed induction generator. In *IEEE Power Engineering Society Summer Meeting 2001*, pages 644–649, 2001.

[15] A. Tapia, G. Tapia, J. X. Ostolaza, and J. R. Sáenz. Modeling and control of a wind turbine driven doubly fed induction generator. *IEEE Trans. Energy Conversion*, 18:194–204, 2003.

Appendix

Proof of Proposition 1 The proof utilizes standard techniques from singular perturbation theory [8]. For, we propose a state realization of (10), taking $x_1 = \tilde{i}_s$, to get

$$\begin{aligned}\dot{x}_1 &= x_2\\ \dot{x}_2 &= x_3\\ \dot{x}_3 &= -(c_1 I_2 + c_2 J_2)x_3 - c_3 x_2 + k_I(c_4^0 x_2 + c_5^0 x_1),\end{aligned}$$

where we have defined $c_4^0 = \frac{c_4}{k_I}$ and $c_5^0 = \frac{c_5}{k_I}$. Denoting $x_{12} = \mathrm{col}(x_1, x_2)$ and $x_{23} = \mathrm{col}(x_2, x_3)$, the last equation can be rewritten as

$$\dot{x}_3 = M x_{23} + k_I A_{12} x_{12},$$

where we defined the fat matrices

$$M = -\left[\begin{array}{cc} c_3 I_2 & c_1 I_2 + c_2 J_2 \end{array}\right], \quad A_{12} = -\left[\begin{array}{cc} c_5^0 I_2 & c_4^0 I_2 \end{array}\right].$$

To obtain the model in the, so–called, standard singular perturbation form we introduce a change of coordinates and a time–scaling. Namely, define the partial coordinate $\eta = x_3 - M x_{12}$ and the time scale $\tau = k_I t$. In the new time scale we obtain

$$\begin{aligned}\frac{d\eta}{d\tau} &= A_{12} x_{12}\\ k_I \frac{dx_{12}}{d\tau} &= A_{21}\eta + A_{22} x_{12},\end{aligned} \qquad (14)$$

where

$$A_{21} = \left[\begin{array}{c} 0 \\ I_2 \end{array}\right], \quad A_{22} = \left[\begin{array}{cc} 0 & I_2 \\ & M \end{array}\right].$$

To complete the proof we invoke Corollary 3.1 of [8], which states that: if the matrices A_{22} and $-A_{12}A_{22}^{-1}A_{21}$ are Hurwitz, then there exists $k_I^M > 0$ such that for all $k_I \in (0, k_I^M]$ the system (14) is asymptotically stable. The matrix A_{22} is the system matrix of the closed–loop with $k_I = 0$. Below Proposition 1 we have shown, using a Lyapunov argument, that this system is asymptotically stable for all $k_P > 0$. Finally, some simple calculations prove that $A_{12}A_{22}^{-1}A_{21} = I_2$, completing the proof.